IOCCG Lecture 2
Optically Shallow Remote Sensing

Dr. Heidi Dierssen
University of Connecticut

Photo: H. Dierssen

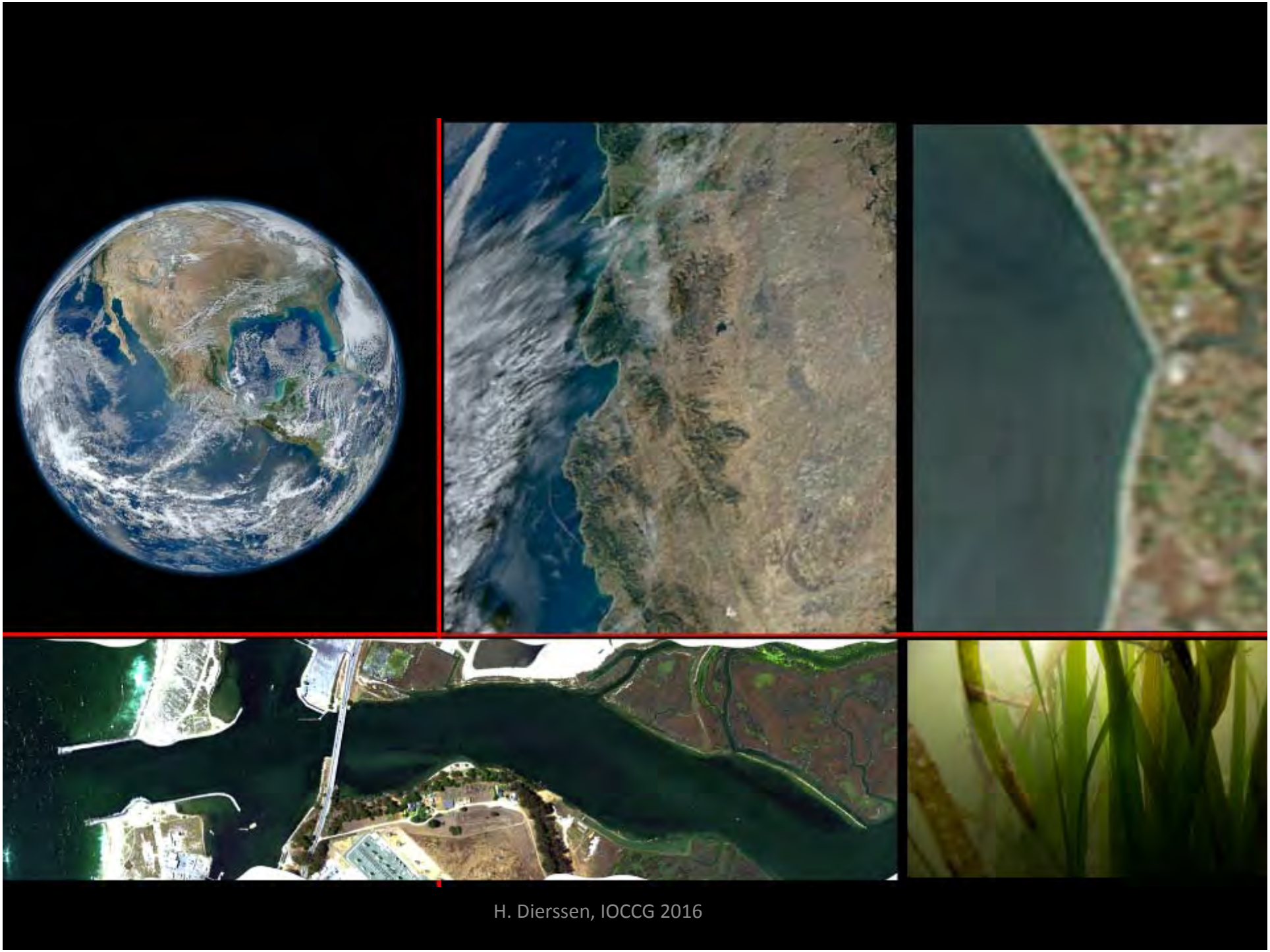
H. Dierssen, IOCCG 2016

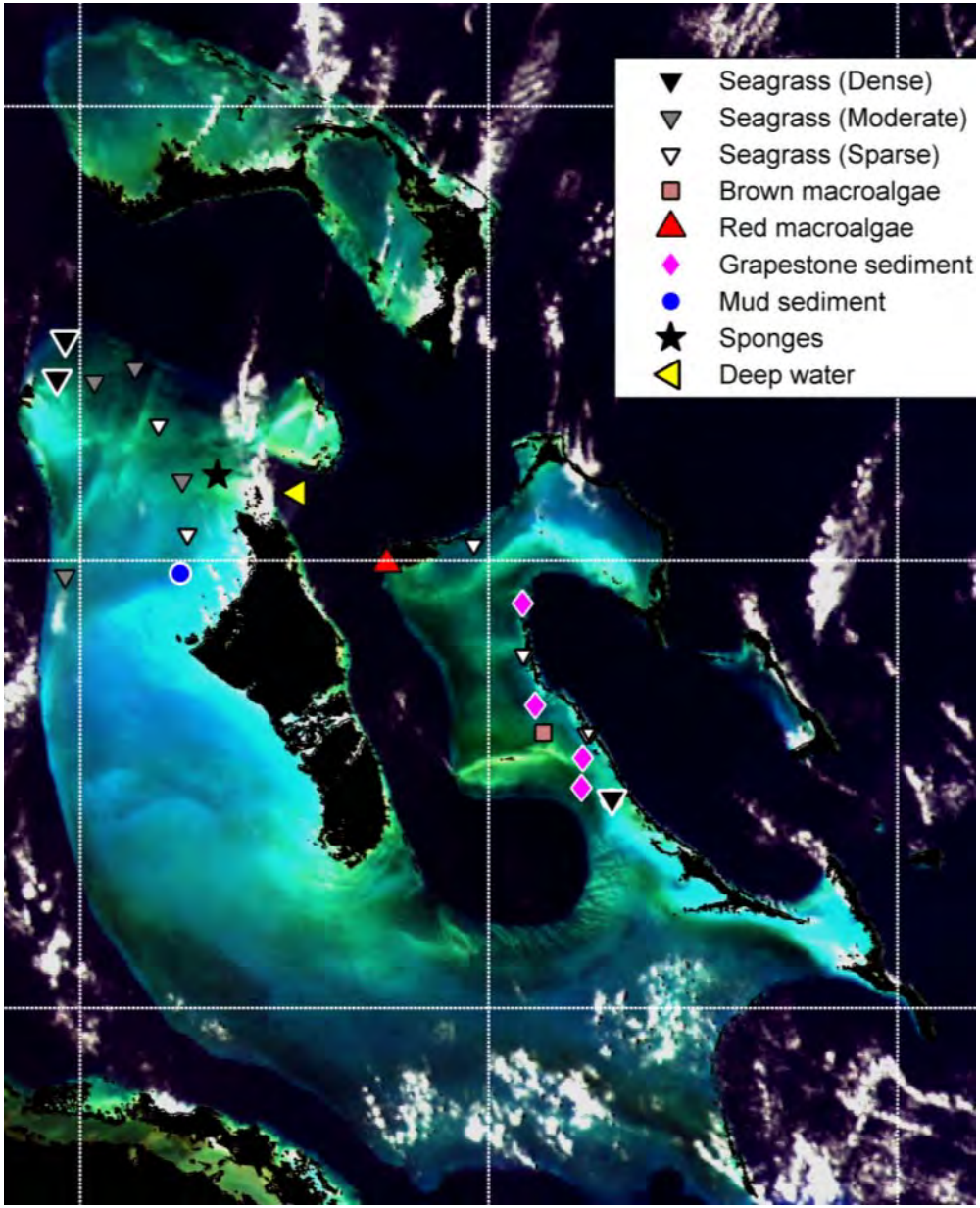

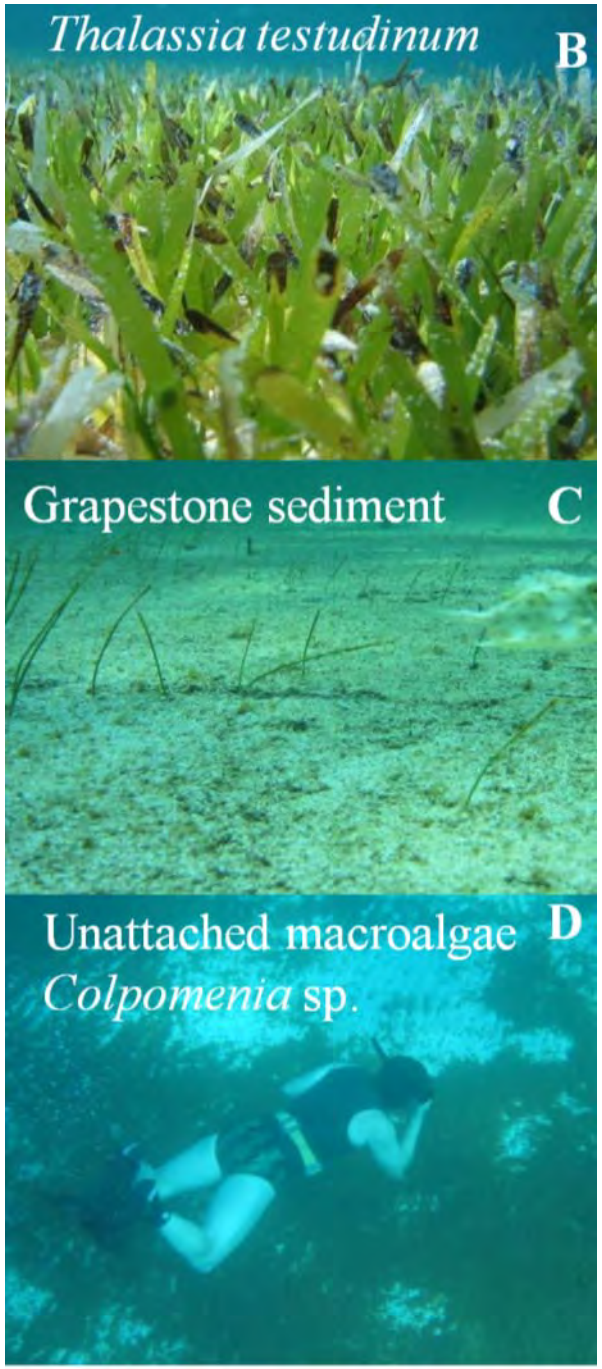

H. Dierssen, IOCCG 2016

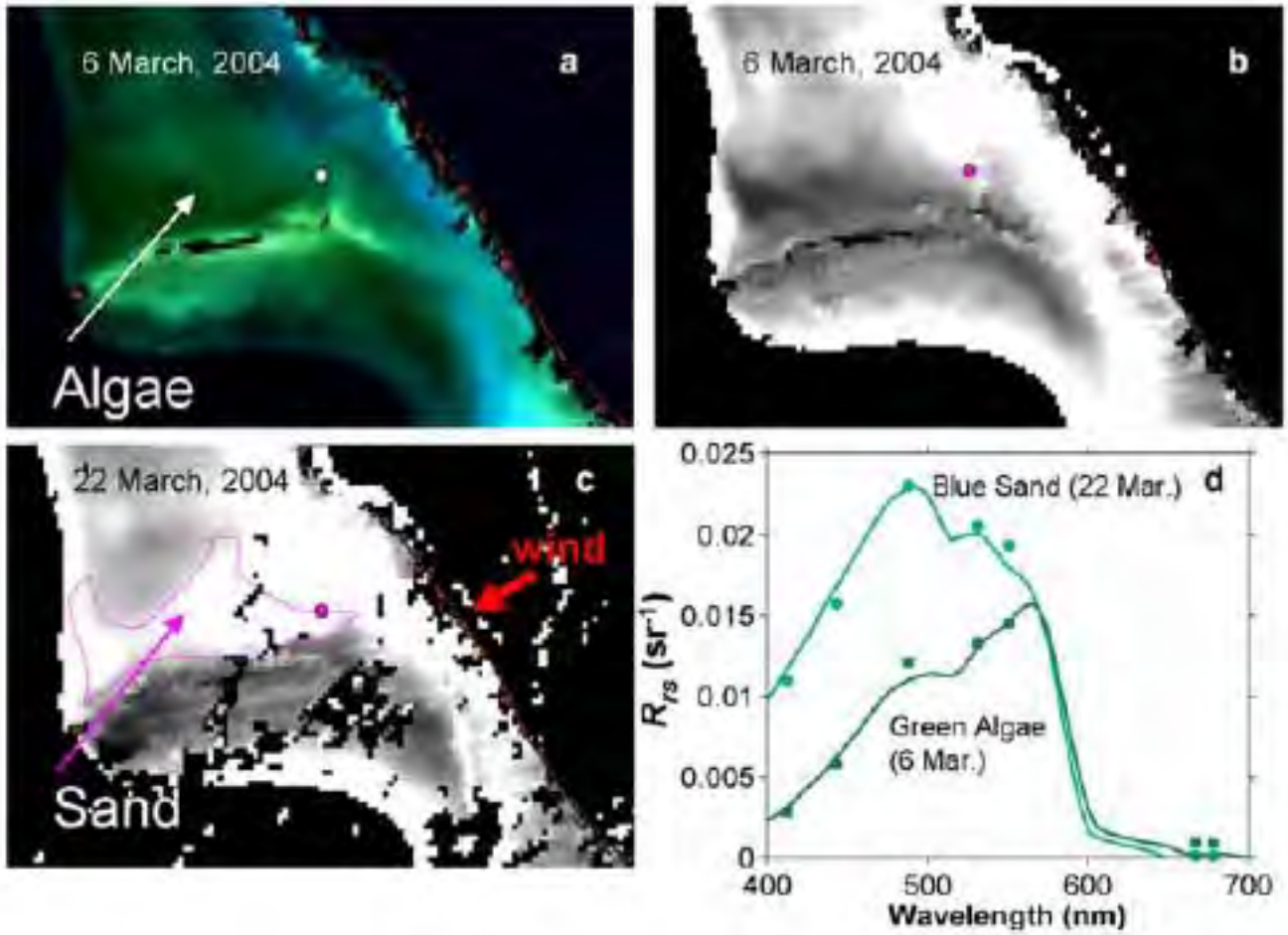

Pulsed export of >7 x10^{10} g of carbon directly to seafloor (negatively buoyant). This is equivalent to the daily carbon flux of phytoplankton biomass in the pelagic tropical North Atlantic and 0.2–0.8% of daily carbon flux from the global ocean.

Dierssen et al. 2009. Geophys. Res. Lett.

GEOPHYSICAL RESEARCH LETTERS, VOL. 36, L04602, doi:10.1029/2008GL036188, 2009

Click Here for Full Article

Potential export of unattached benthic macroalgae to the deep sea through wind-driven Langmuir circulation

H. M. Dierssen,[1] R. C. Zimmerman,[2] L. A. Drake,[2,3] and D. J. Burdige[2]

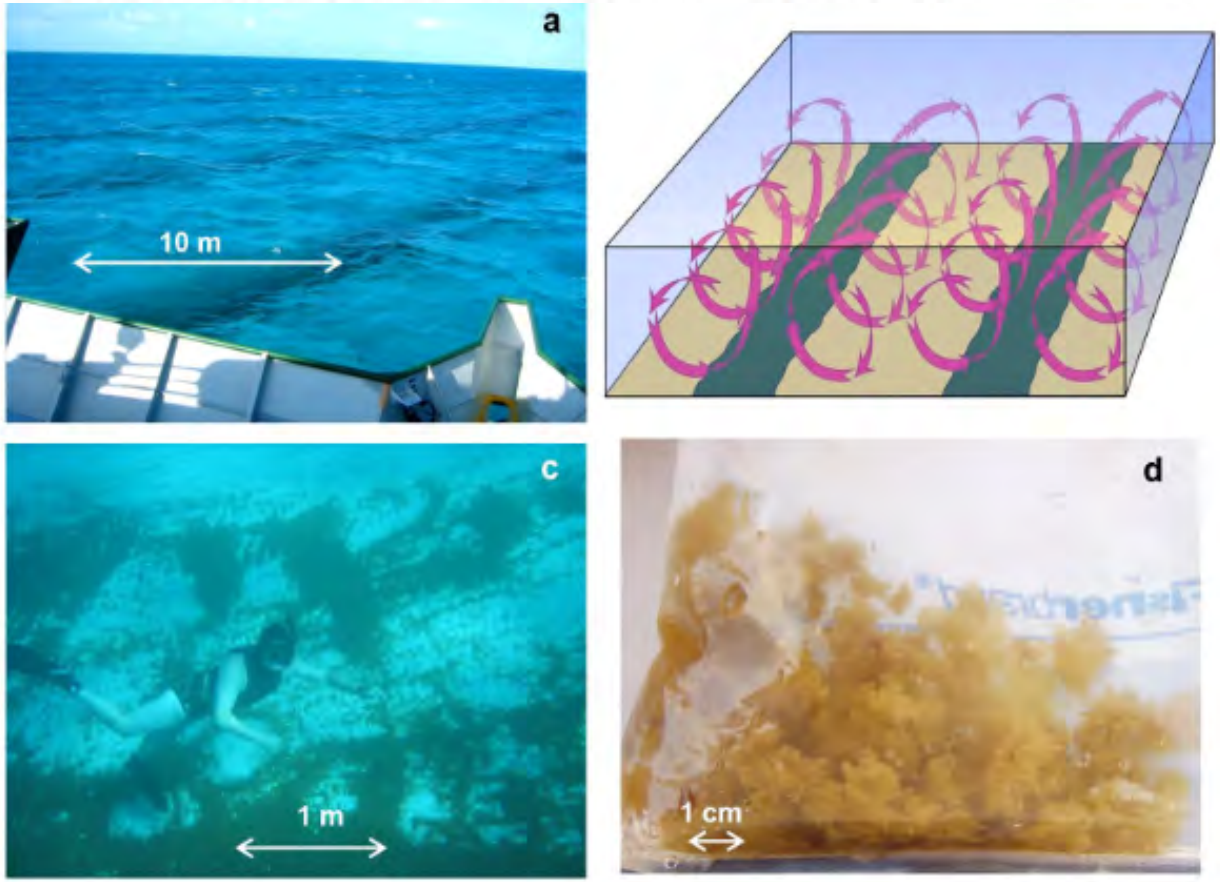

H. Dierssen, IOCCG 2016

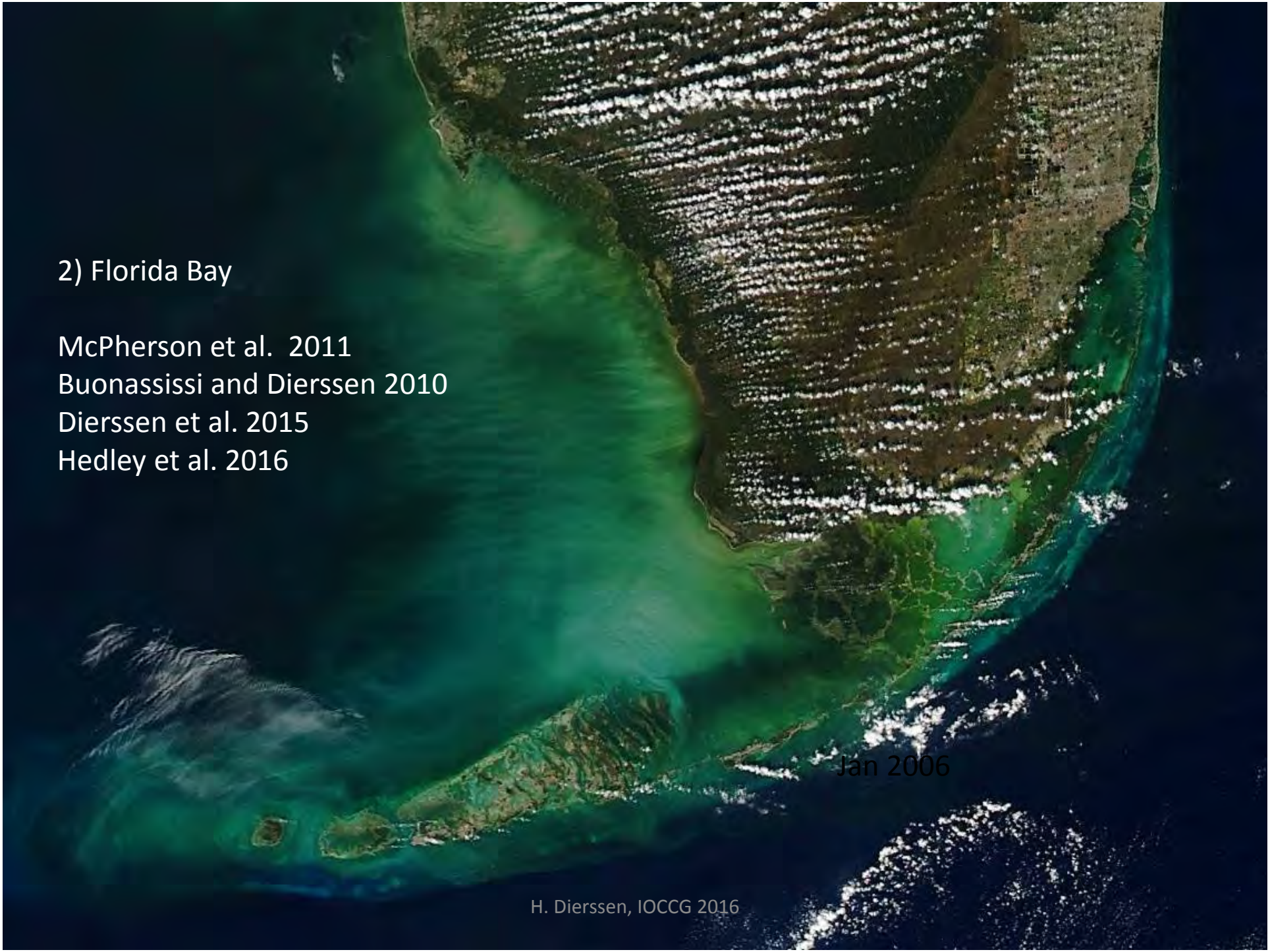
2) Florida Bay
McPherson et al. 2011
Buonassissi and Dierssen 2010
Dierssen et al. 2015
Hedley et al. 2016
Jan 2006
H. Dierssen, IOCCG 2016

Figure adapted from Eric Louchard

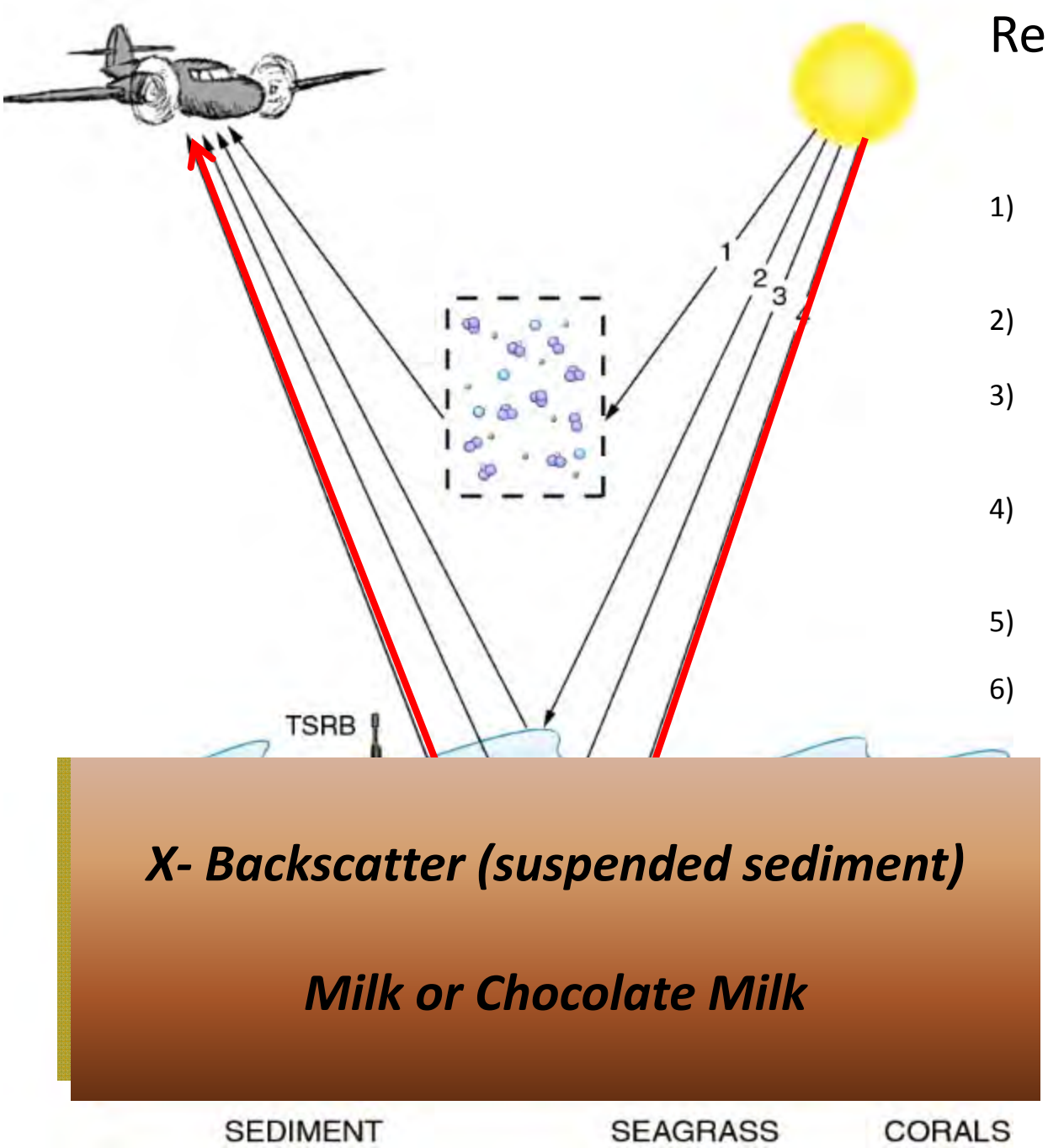

Remote Sensing of ***Optically Shallow*** Water

1) Benthic Reflectance (R_b)
   Canopy and Sediment

2) Water Column Optical Properties

3) Water Depth (H) and
   Canopy Height

4) Air-water Interface
   Waves, Glint and Whitecaps

5) Atmosphere -- aerosols

6) Tools to survey
   -Sensors
   -Radiative Transfer Models
   Hydrolight (Mobley)
   3D canopy model (Hedley)

X- Backscatter (suspended sediment)

Milk or Chocolate Milk

H. Dierssen, IOCCG 2016

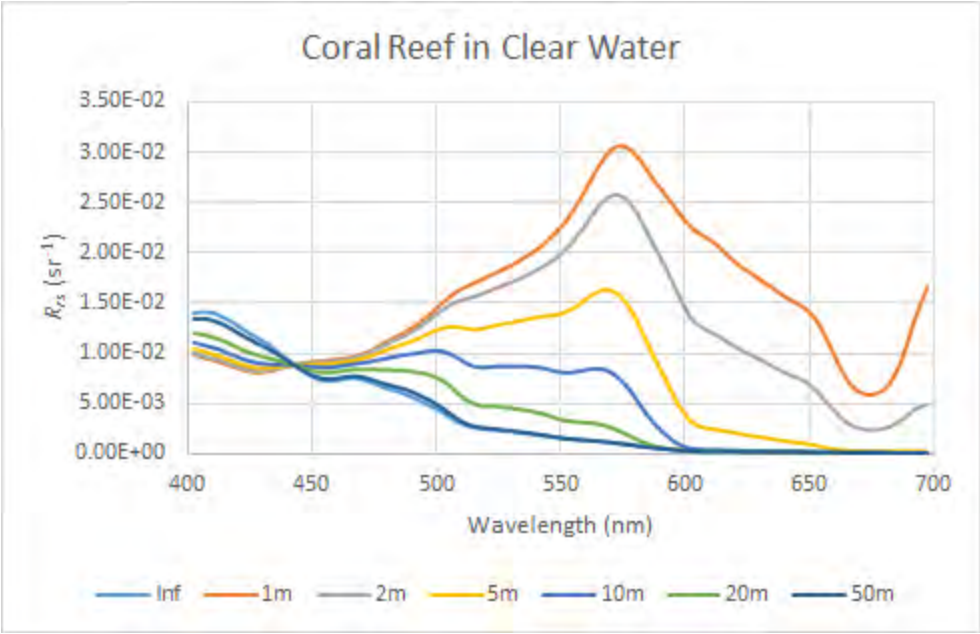

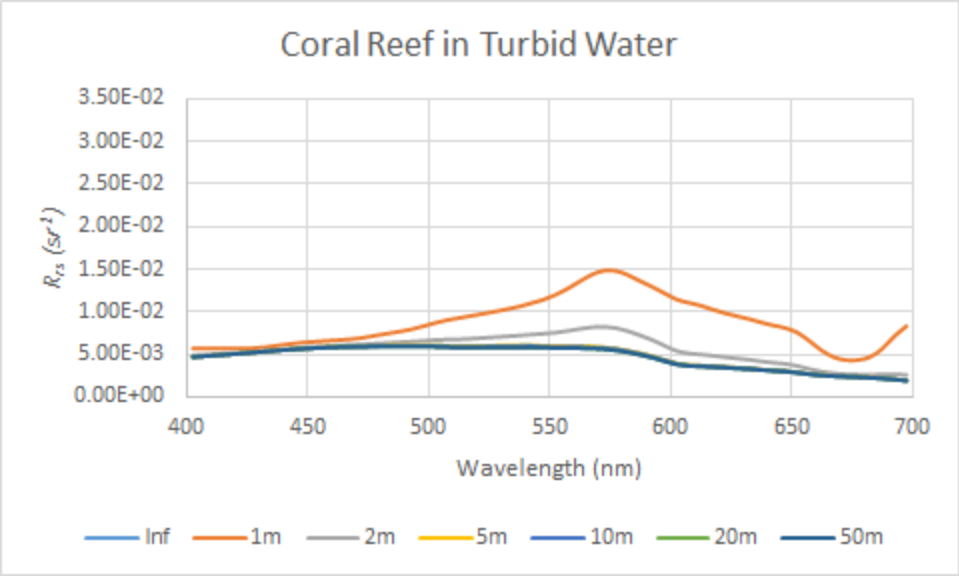

H. Dierssen, IOCCG 2016

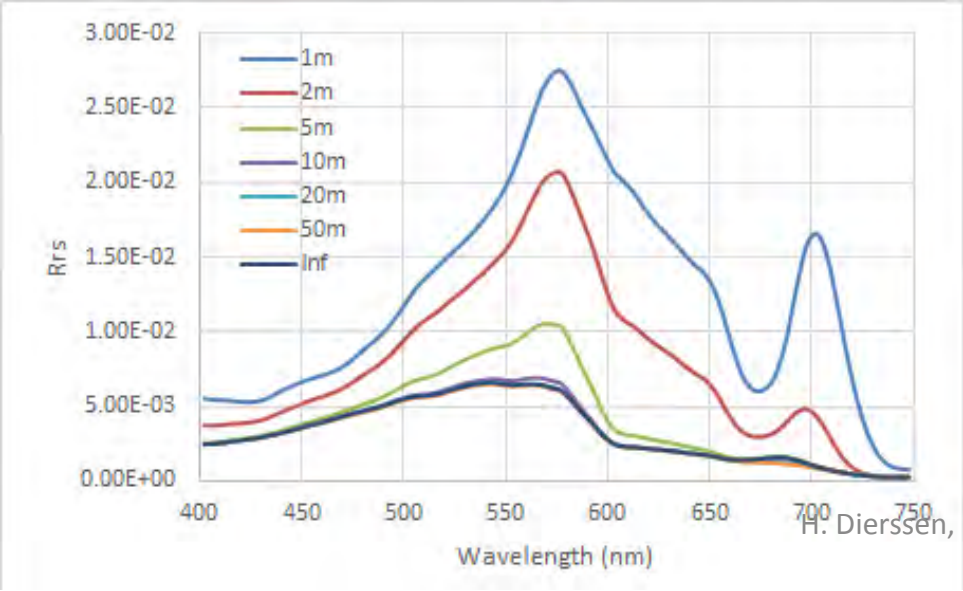

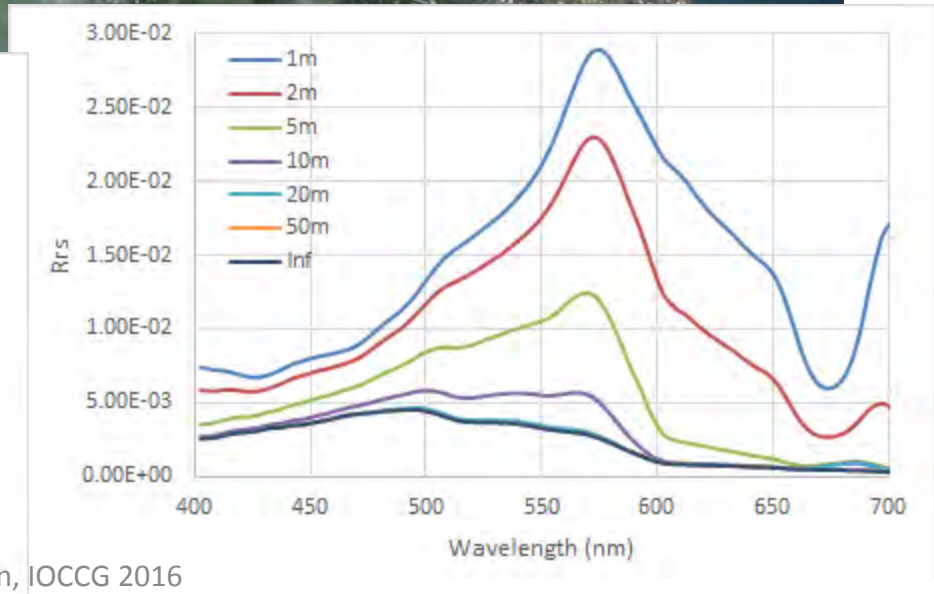

H. Dierssen, IOCCG 2016

Requirements for Optically Shallow Remote Sensing

Spectral Resolution

- Hyperspectral is generally required to differentiate bottom types (e.g., coral vs. macroalgae (Hochberg and Atkinson 2000)
- Otherwise, you need *a priori* knowledge of site and limited in what you can differentiate (e.g., reef extent)

Spatial Resolution

- Depends on science question
- 1 – 10 m Aircraft or In-water AUVs
- 30-100 m Hyperspectral Satellites
- 200-1000 m Ocean color satellites

Image Processing

- Removal of sun glint
- Atmospheric correction
- Water column correction

Ancillary Data

- Field data
  - Rrs
  - IOPs
  - Benthic cover
  - Aerosols (sun photometer)
- Bathymetry

H. Dierssen, IOCCG 2016

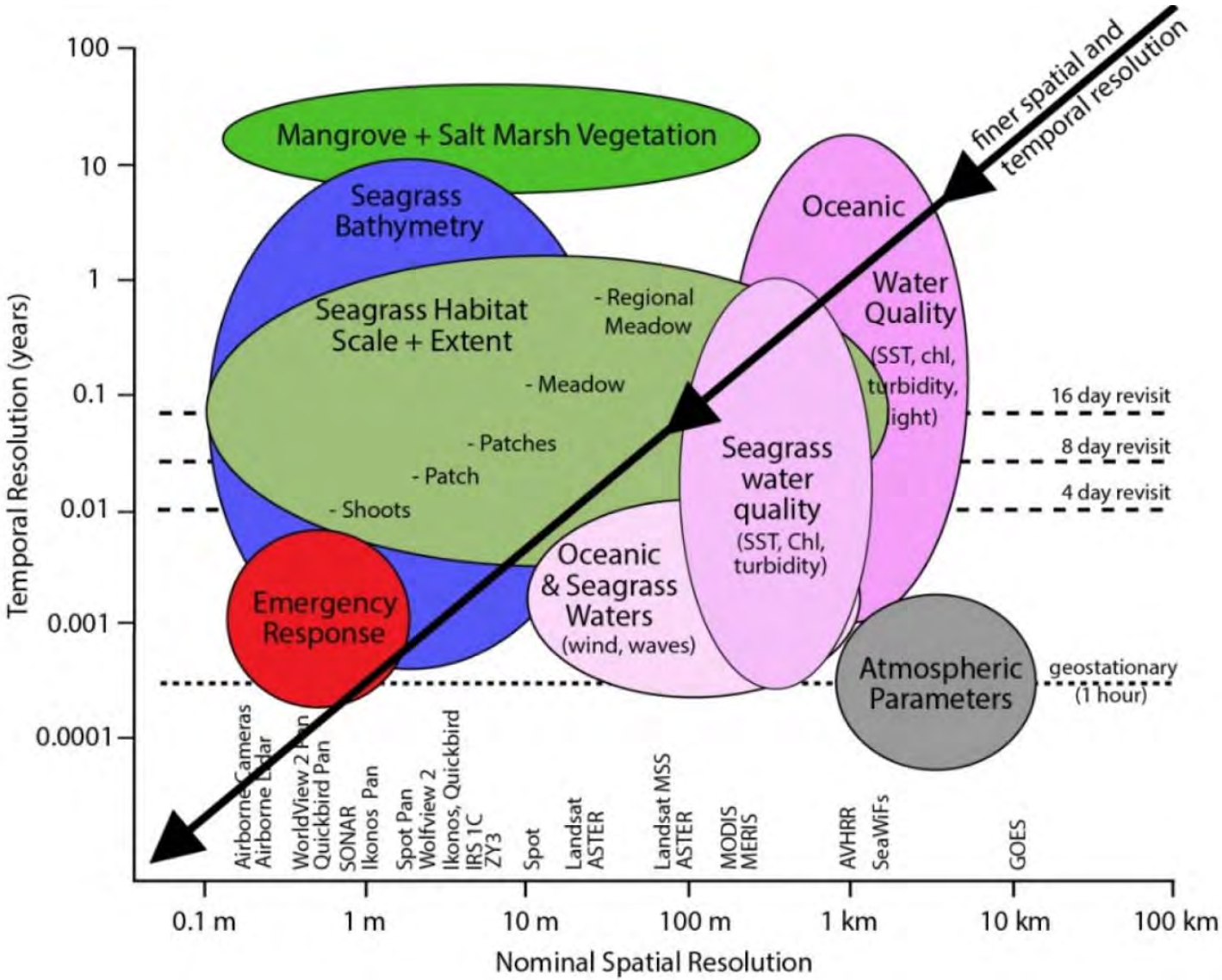

H. Dierssen, IOCCG 2016

Hedley et al. 2016

Case Study with the Airborne Hyperspectral PRISM Sensor

PRISM

Portable Remote Imaging Spectrometer

Built in 2012 by NASA JPL funded by NASA Ocean Biology and Biogeochemistry to address challenges of coastal remote sensing. Hyperspectral (350-1050 nm) ,Integrated on Twin Otter Platform for <1 m pixels and also on ER2 or GV5 for 10 m pixels.

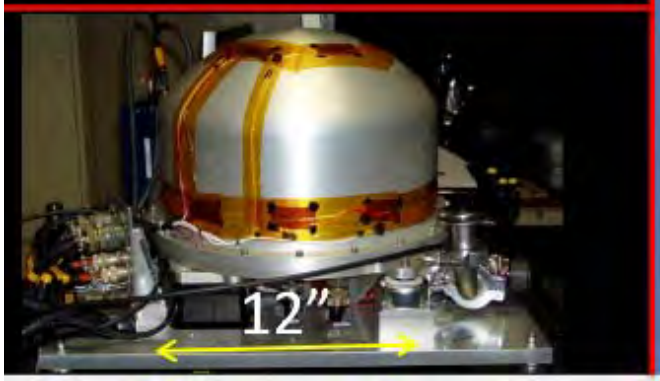

Photo: E. Heupel

H. Dierssen, IOCCG 2016

Portable Remote Imaging SpectroMeter (PRISM): NASA Coastal Applications

Spectral	Range	**350-1050 nm**
	Sampling	**2.85 nm**
	Resolution (FWHM)	3.5 nm
	Calibration uncertainty	< 0.1nm
Spatial	Field of view	30.7°
	Instantaneous FOV sampling	0.882 mrad
	IFOV resolution (FWHM)	0.97 mrad
	Cross-track spatial pixels	608
	Ground resolution	**0.35 – 20 m**
Radiometric	Range	0 to max. beach R
	Sampling	**14 bit**
	Stability	>99%
	Calibration uncertainty	<2%
	SNR	**2000 @450 nm***
	Polarization variation:	**< 1%**
Uniformity	Spectral cross-track uniformity	**>95%**
	Spectral IFOV mixing uniformity	**>95%**

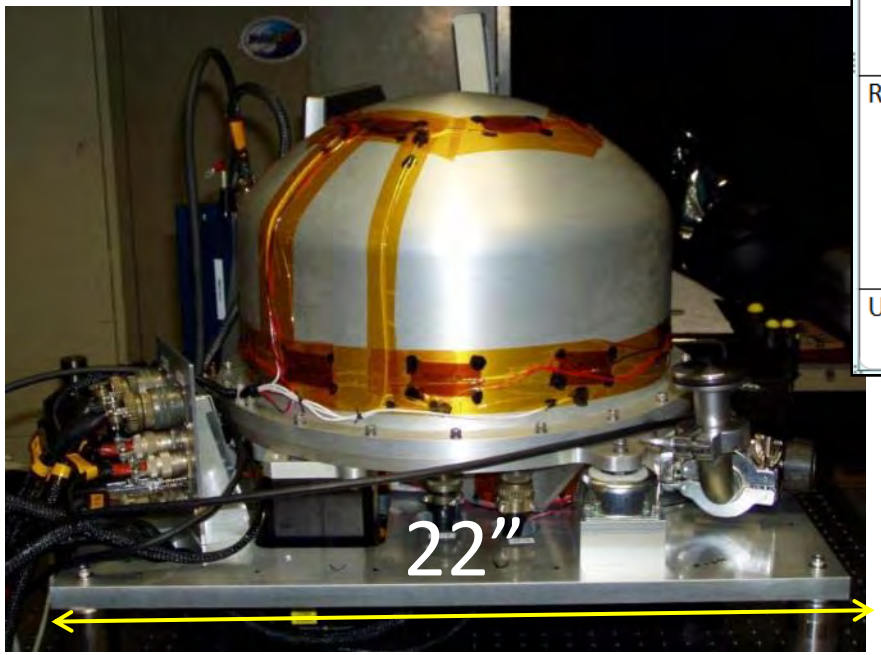

Mouroulis et al. 2013

Tackling Sun Glint

- Can align overflights into or out of sun
  - Avoid Across-track glint

- Remove glint
  - Empirical linear relationships
  - Wave features removed baseline at 980 nm

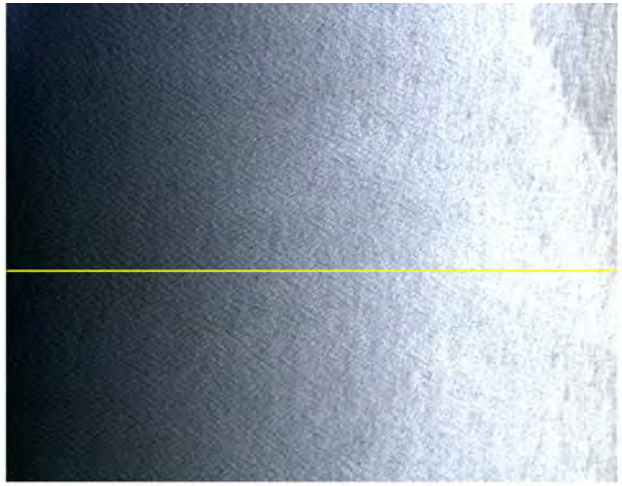

Figure 3.2-3 AVIRIS scene f000418t01p03_r01. Yellow line shows location of cross-track sample analyzed in Figure 3.2-4.

Figure 1.2-4 Quickbird scene of Bermuda. (Left) Wide-area scene to provide context. Yellow box shows location of close-up detail scene. (Right) Close-up scene to show detail of glint distribution. This scene illustrates a nearly stochastic sea surface; wind chop is convolved with small surface gravity waves. In this case, sensor view angle also increases sunglint intensity.

Photos: Hyspiri sunglint subgroup report.

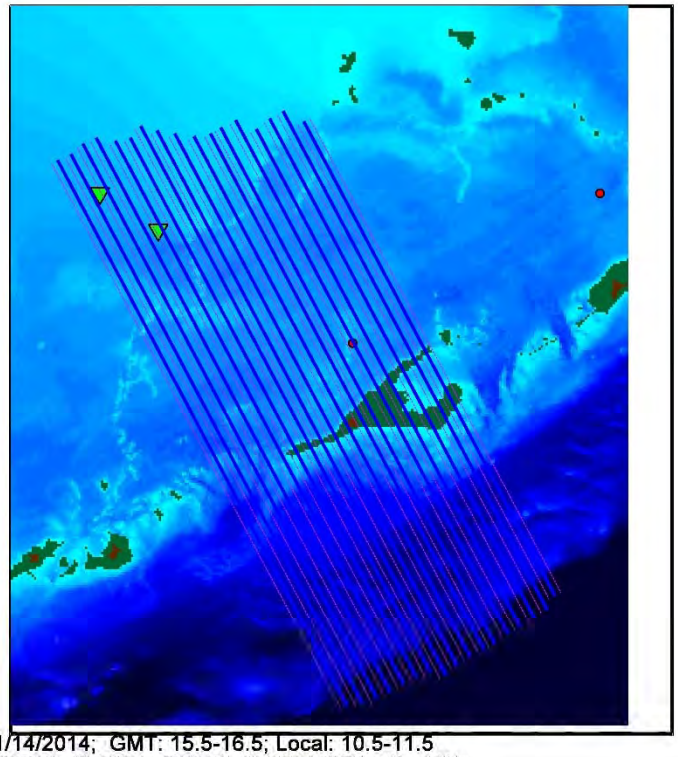

Date: 1/14/2014; GMT: 15.5-16.5; Local: 10.5-11.5

Line 1: [24.7564N, -80.7532W] to [24.9115N, -80.8436W]; 19.50 km; Time 0.13 hr

Line 2: [24.7518N, -80.756W] to [24.9148N, -80.8511W]; 20.51 km; Time 0.14 hr

Line 3: [24.7484N, -80.7602W] to [24.9124N, -80.8559W]; 20.64 km; Time 0.14 hr

Line 4: [24.746N, -80.7656W] to [24.909N, -80.8607W]; 20.52 km; Time 0.14 hr

Line 5: [24.7439N, -80.7702W] to [24.9119N, -80.8682W]; 21.14 km; Time 0.14 hr

Line 6: [24.7401N, -80.7747W] to [24.9095N, -80.8735W]; 21.31 km; Time 0.14 hr

Line 7: [24.7384N, -80.7786W] to [24.9076N, -80.8773W]; 21.28 km; Time 0.14 hr

Line 8: [24.7362N, -80.7838W] to [24.9066N, -80.8831W]; 21.43 km; Time 0.14 hr

Line 9: [24.7332N, -80.7884W] to [24.9076N, -80.8901W]; 21.94 km; Time 0.15 hr

Line 10: [24.73N, -80.7924W] to [24.9086N, -80.8965W]; 22.47 km; Time 0.15 hr

Line 11: [24.731N, -80.798W] to [24.91N, -80.9024W]; 22.52 km; Time 0.15 hr

Line 12: [24.7295N, -80.8031W] to [24.9061N, -80.9061W]; 22.23 km; Time 0.15 hr

Line 13: [24.7271N, -80.8077W] to [24.9052N, -80.9114W]; 22.40 km; Time 0.15 hr

Line 14: [24.7245N, -80.8125W] to [24.9061N, -80.9184W]; 22.85 km; Time 0.15 hr

Line 15: [24.7223N, -80.8172W] to [24.9042N, -80.9232W]; 22.88 km; Time 0.15 hr

Line 16: [24.7211N, -80.8227W] to [24.9008N, -80.9275W]; 22.61 km; Time 0.15 hr

Total Dist.: 368.70 km; Min. Time: 2.5; Azimuth: 152, SZA: 51.3

Line 17: [24.7202N, -80.8281W] to [24.8989N, -80.9323W]; 22.47 km; Time 0.15 hr

Can be helpful to develop hourly flight lines or morning/ afternoon lines to avoid sun glint

H. Dierssen, IOCCG 2016

PRISM Atmospheric Correction Procedure

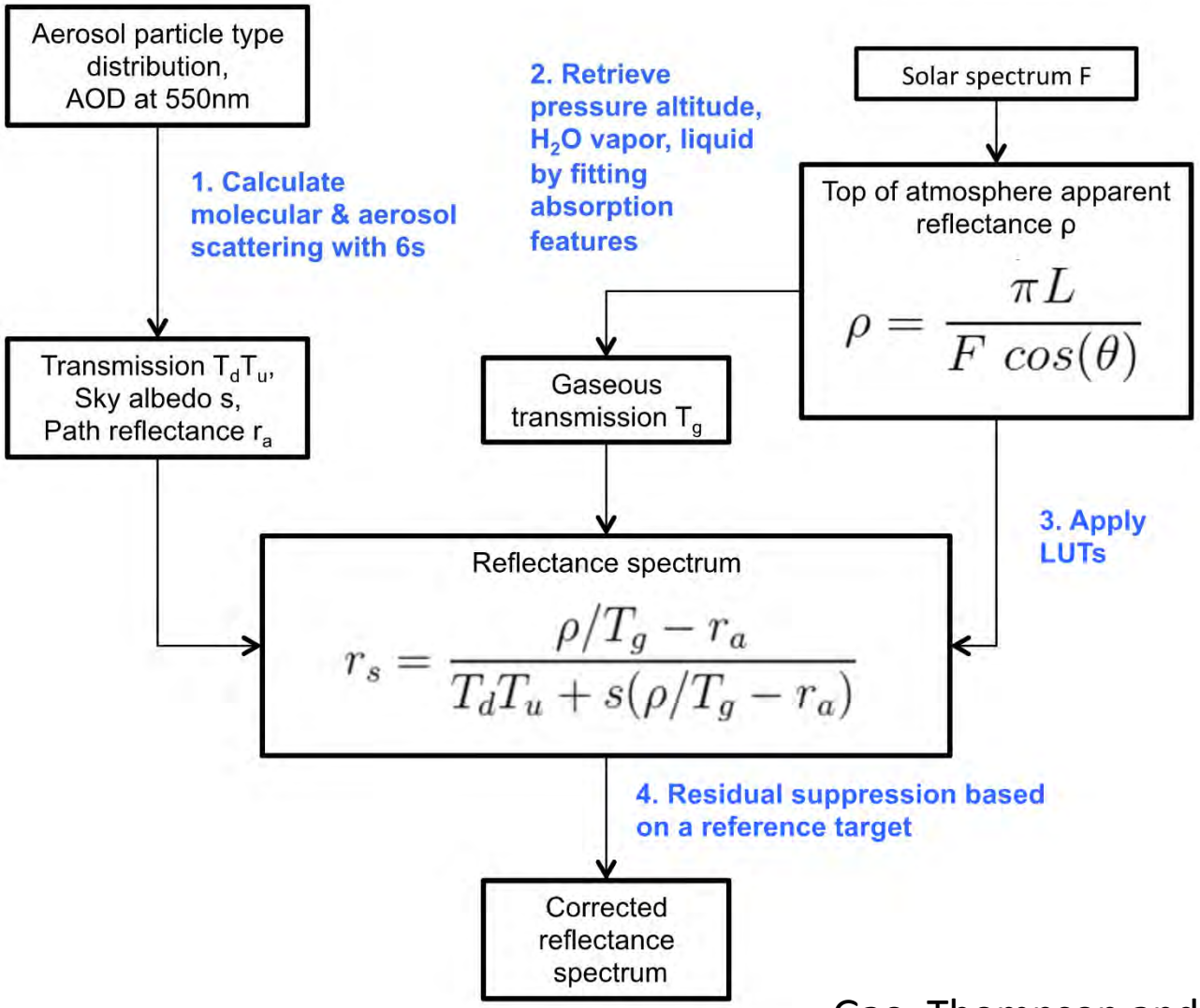

Gao, Thompson and Gierach 2016

H. Dierssen, IOCCG 2016

Methods for Remote Sensing

- Empirical -- pick known endmembers, thresholds, waveband ratios, etc…
- Look Up Table (LUT)
  - Propagate benthic reflectance in Hydrolight
    - different depths and water IOPs
  - Spectral matching of Rrs to a LUT library of Rrs

- Semi-analytical Inversion Modeling

  Majority based on HOPE model

  (Lee et al. 1998,1999)
    - P, G, X, B, H
    - B=Benthic Reflectance
    - H=Water depth

- P=*a_phy* (440)
- G=*a_g*(440)
- X=b_{bp}(550)
- Slope parameters
  - Scdom= 0.015
  - Y=0.5

$$b_{bp}(\lambda) = X\left(\frac{550}{\lambda}\right)^{Y}$$

$$a_g(\lambda) = G\, e^{-S(\lambda-440)}$$

H. Dierssen, IOCCG 2016

Interpretation of hyperspectral remote-sensing imagery by spectrum matching and look-up tables

Curtis D. Mobley, Lydia K. Sundman, Curtiss O. Davis, Jeffrey H. Bowles,
Trijntje Valerie Downes, Robert A. Leathers, Marcos J. Montes, William Paul Bissett,
David D. R. Kohler, Ruth Pamela Reid, Eric M. Louchard, and Arthur Gleason

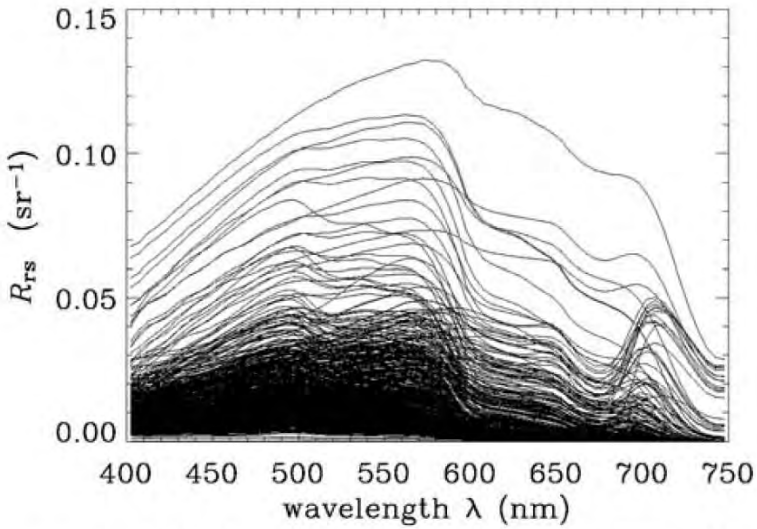

Fig. 8. Randomly chosen selection of 2% of the 41,591 EcoLUT-generated R_{rs} spectra in the LUT database (832 spectra plotted).

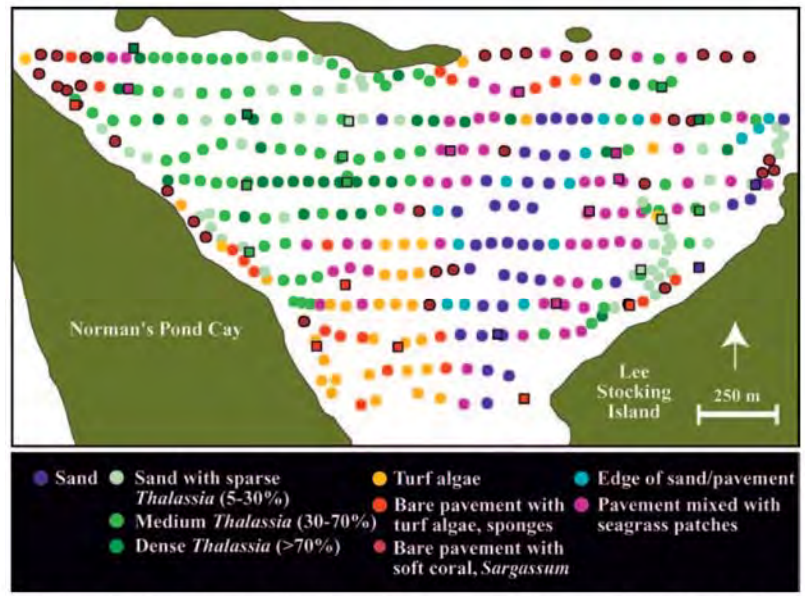

6. Bottom classification based on diver observation (squares) and video recorded from a small boat (circles).

H. Dierssen, IOCCG 2016

Assumptions and Variations for Inversion Model HOPE

- Initial assumptions can be tuned
- Models vary in terms of:
  - Retrieve mixture of benthos
  - Retrieve more water column properties
- Can propagate uncertainty estimates

$$P = 0.05 \left(\frac{R_{rs}(440)}{R_{rs}(550)} \right)^{-1.7}$$

$$G = 1.5\,P$$

$$X = 8\,R_{rs}(660)$$

$$B = 4\,R_{rs}(490)$$

$$H = \frac{1}{6\,P}$$

H. Dierssen, IOCCG 2016

Remote Sensing of Environment 174 (2016) 134–147

Contents lists available at ScienceDirect

Remote Sensing of Environment

journal homepage: www.elsevier.com/locate/rse

A physics-based method for the remote sensing of seagrasses

John Hedley [a,*], Brandon Russell [b], Kaylan Randolph [b], Heidi Dierssen [b]

[a] Environmental Computer Science Ltd., Raymond Penny House, Tiverton, Devon EX16 6LR, United Kingdom
[b] Department of Marine Sciences, University of Connecticut, Groton, CT 06340, USA

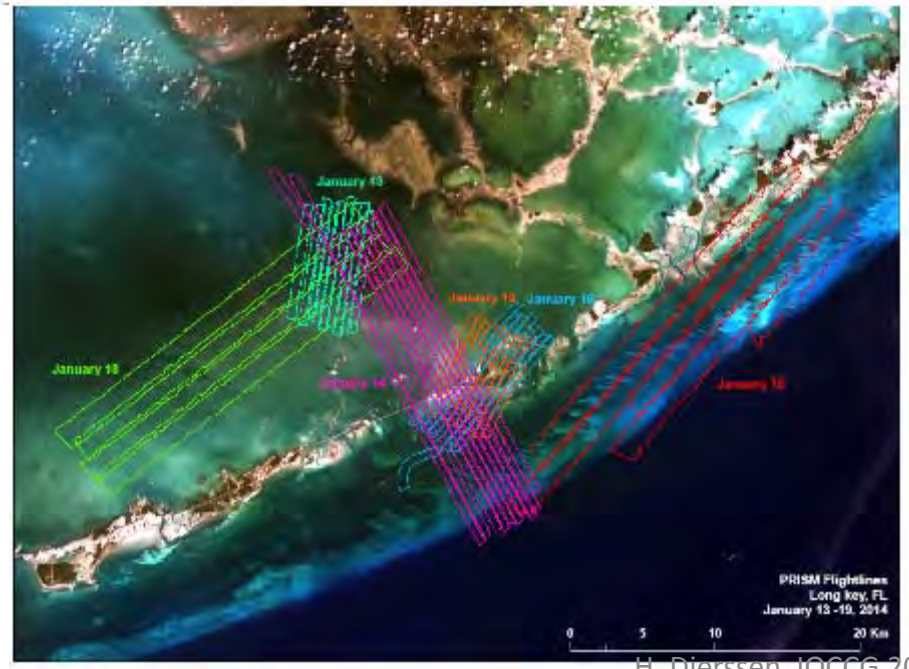

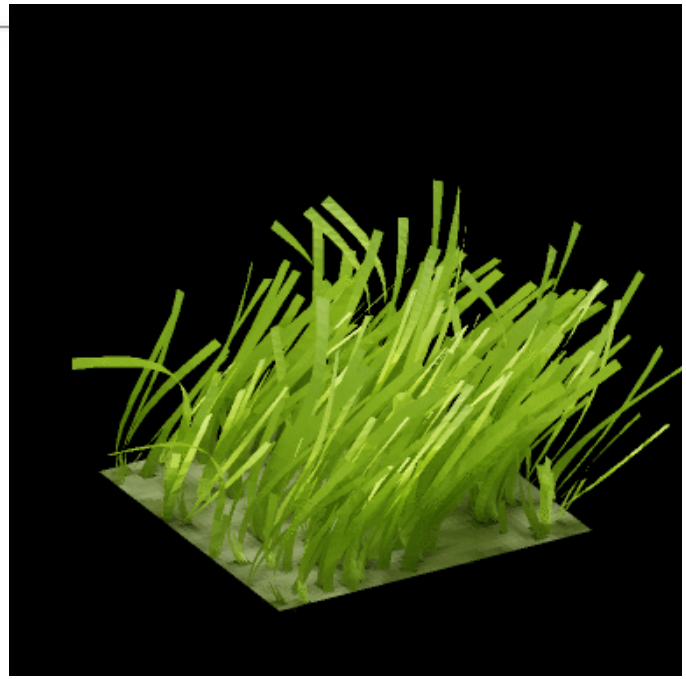

H. Dierssen, IOCCG 2016

Image analysis compared to in-situ LAI data

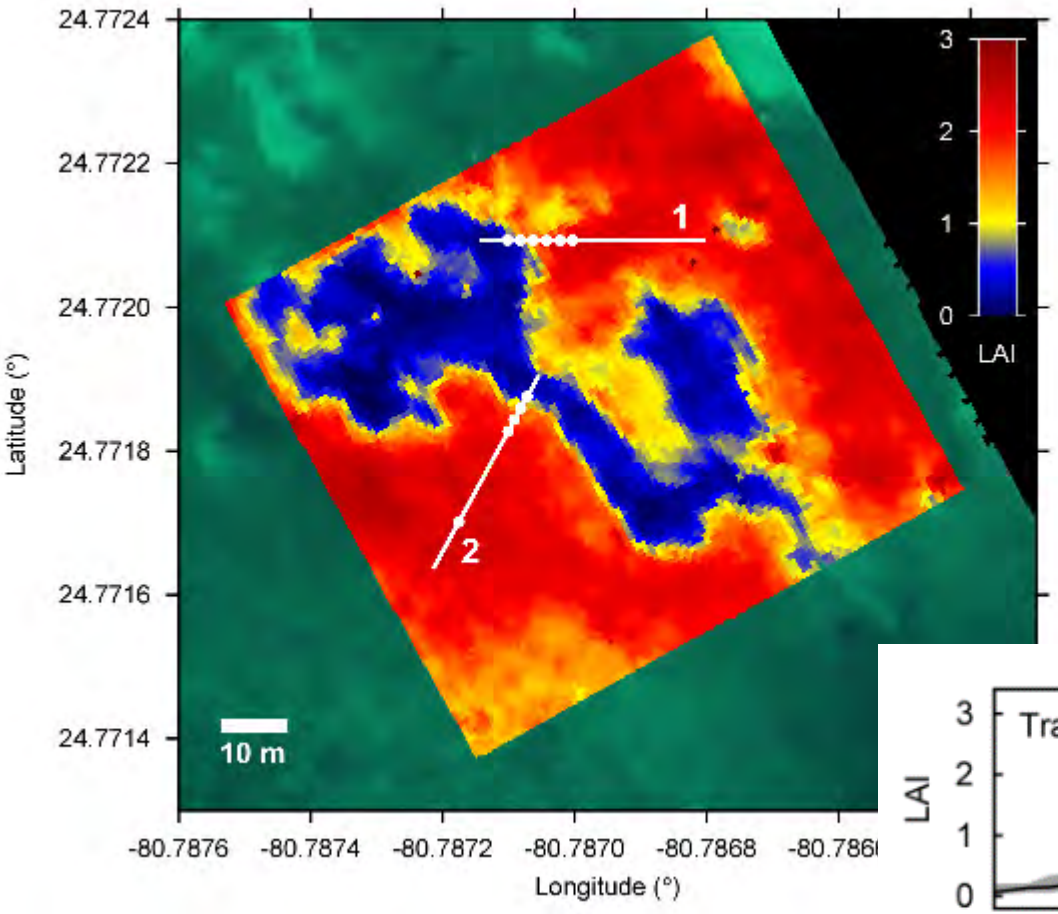

- Basic pattern matches in-situ data
- Spatial variation in in-situ LAI is higher
- Need for more appropriate sampling regimes for meter-scale imagery
- Can convert to CARBON storage

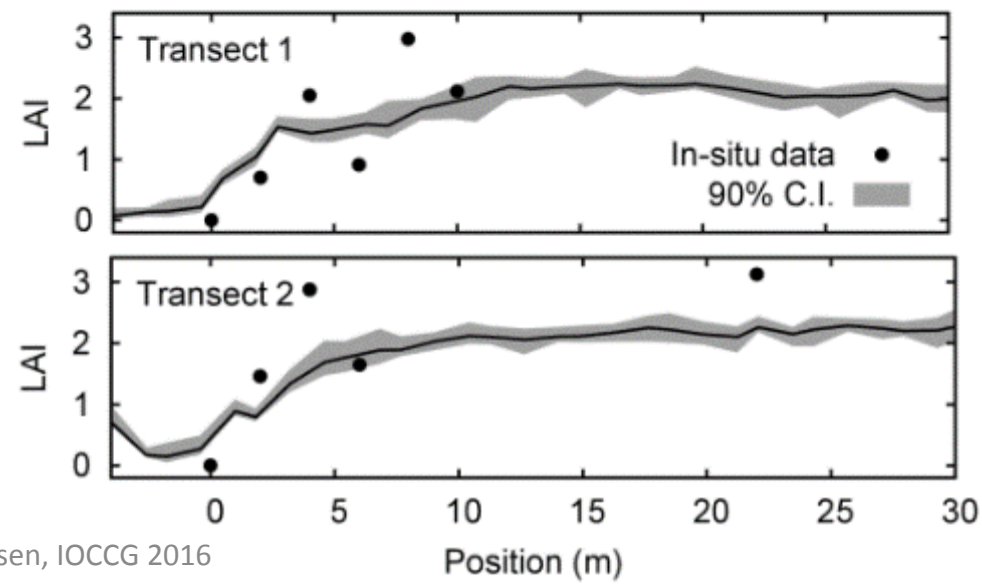

Hedley et al. Submitted. Remote Sens. Environ.

How well does the model work in Turbid Water? Example provided

Eric Heupel Photography
Dierssen 2013 SPIE

For deeper habitats, imagers can be mounted on Remotely Operated Vehicles

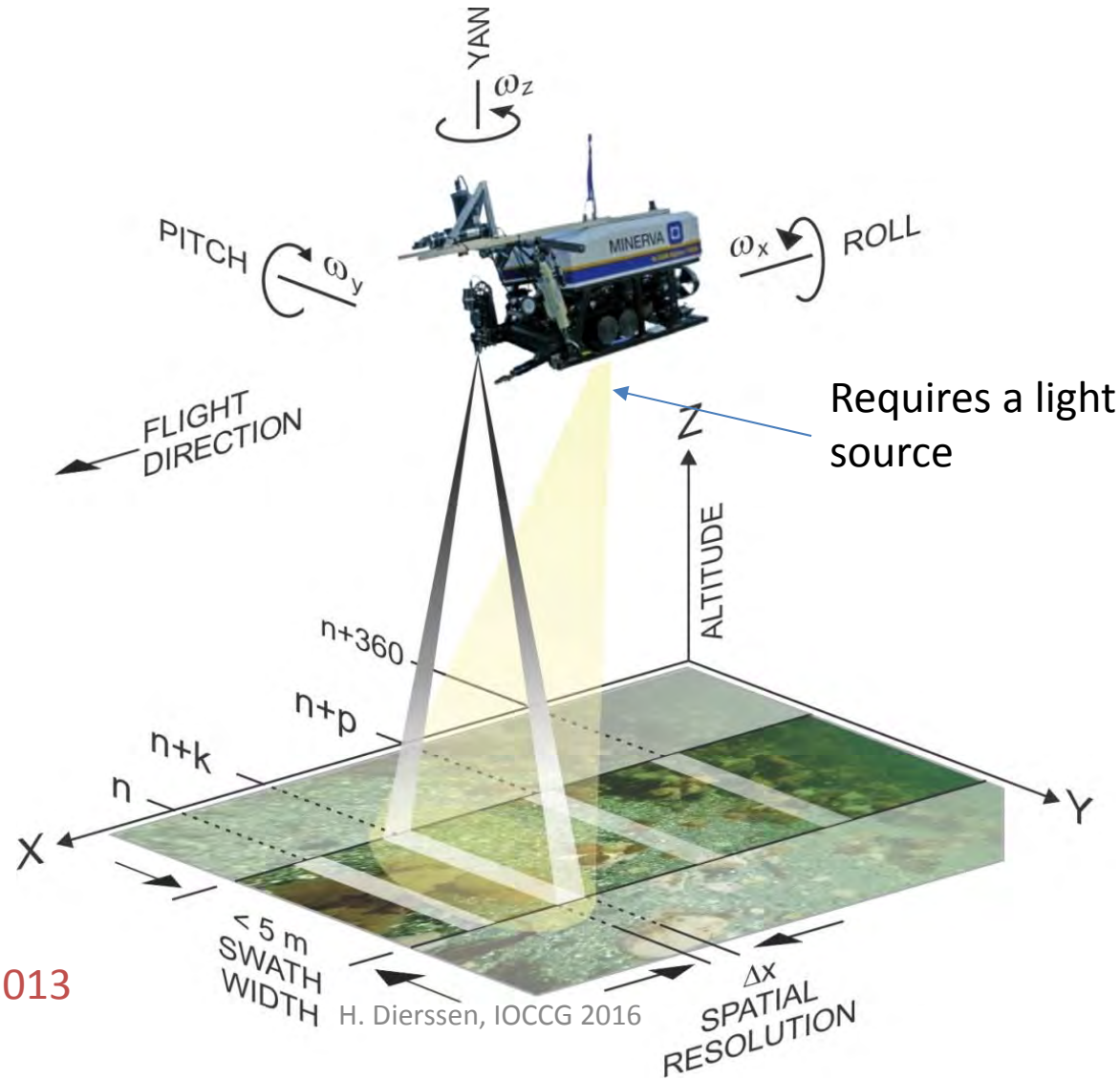

Requires a light source

Johnsen et al. 2013

H. Dierssen, IOCCG 2016

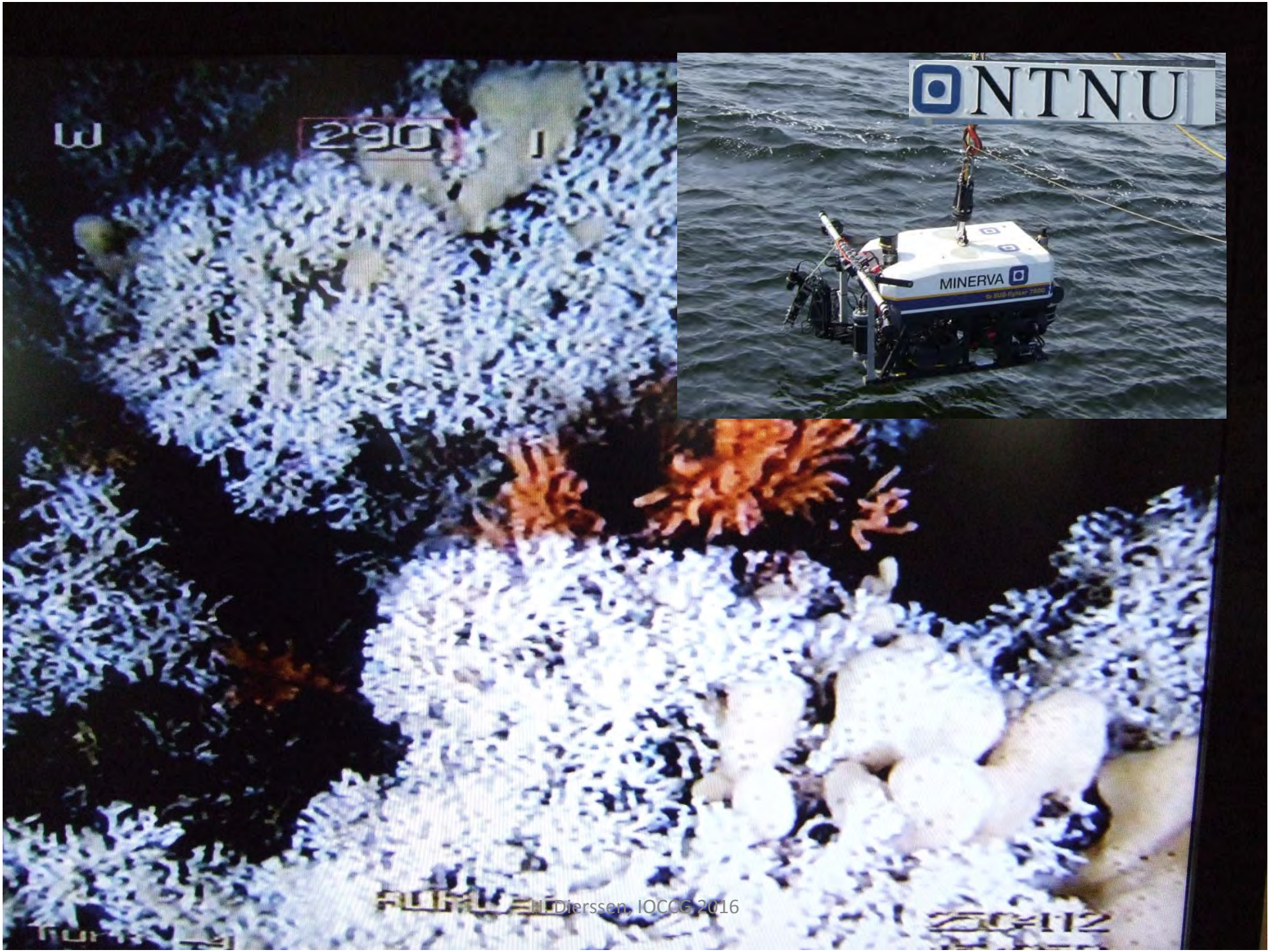
W
290
J
NTNU
MINERVA
H. Dierssen, IOCCG 2016

About CORAL

It is estimated that 33-50% of coral reefs worldwide have been largely or completely degraded (International Society for Reef Studies Consensus Statement, October 2015). Yet the data supporting these predictions are surprisingly sparse, and thereby their relation to the environment is unclear. The COral Reef Airborne Laboratory (CORAL) will pave the way to better predict the future of this global ecosystem and steward them through global change by addressing the question: **What is the relationship between coral reef condition and biogeophysical forcing parameters?** Over a three-year campaign, CORAL will:

Objective 1. Measure the condition of representative coral reefs across the global range of reef biogeophysical values. The primary indicators for coral reef condition are benthic cover (ratio of coral, algae, and sand), primary productivity, and calcification.

H. Dierssen, IOCCG 2016

PRISM Data Dissemination

http://prism.jpl.nasa.gov/alt_locator/

Concluding thoughts

- Great strides in optically shallow remote sensing
  - Better Sensors
  - Better Algorithms
  - Hopefully will become cheaper for different applications
- Lots of exciting research yet to be done
- Go out and bring ocean spectroscopy to the community:
  - physiologists, benthic ecologists and coastal decision makers

H. Dierssen, IOCCG 2016

Select References

Dekker, A. G., S. R. Phinn, J. Anstee, and others. 2011. Intercomparison of shallow water bathymetry, hydro-optics, and benthos mapping techniques in Australian and Caribbean coastal environments. Limnol Ocean. Methods **9**: 396–425.

Dierssen, H. M. 2010. Benthic ecology from space: optics and net primary production in seagrass and benthic algae across the Great Bahama Bank. Mar Ecol Prog. Ser **411**: 1–15. doi:10.3354/meps08665

Dierssen, H. M., R. C. Zimmerman, L. A. Drake, and D. J. Burdige. 2009. Potential export of unattached benthic macroalgae to the deep sea through wind-driven Langmuir circulation. Geophys. Res. Lett. **36**: L04602.

Hedley, J., and S. Enrıquez. 2010. Optical properties of canopies of the tropical seagrass Thalassia testudinum estimated by a three-dimensional radiative transfer model. Limnol Ocean. **55**: 1537–1550.

Hochberg, E., and M. Atkinson. 2000. Spectral discrimination of coral reef benthic communities. Coral Reefs **19**: 164–171.

Johnsen, G., Z. Volent, H. M. Dierssen, and others. 2013. Underwater hyperspectral imagery to create biogeochemical maps of seafloor properties, *In* Subsea Optics and Imaging. Woodhead Publishing.

Select References

Lee, Z., K. L. Carder, C. D. Mobley, R. G. Steward, and J. S. Patch. 1999. Hyperspectral Remote Sensing for Shallow Waters. 2. Deriving Bottom Depths and Water Properties by Optimization. Appl. Opt. **38**: 3831–3843.

Mobley, C. D., L. K. Sundman, C. O. Davis, and others. 2005. Interpretation of hyperspectral remote-sensing imagery by spectrum matching and look-up tables. Appl. Opt. **44**: 3576–3592.

Mobley, C. D., H. Zhang, and K. J. Voss. 2003. Effects of optically shallow bottoms on upwelling radiances: Bidirectional reflectance distribution function effects. Limnol. Oceanogr. **48**: 337–345.

Mouroulis, P., B. Van Gorp, R. O. Green, and others. 2014. Portable Remote Imaging Spectrometer coastal ocean sensor: Design, characteristics, and first flight results. Appl. Opt. **53**: 1363–1380.

Russell, B. J., H. M. Dierssen, T. C. LaJeunesse, K. D. Hoadley, M. E. Warner, D. W. Kemp, and T. G. Bateman. 2016. Spectral Reflectance of Palauan Reef-Building Coral with Different Symbionts in Response to Elevated Temperature. Remote Sens. **8**: 164.

Torres-Pérez, J. L., L. S. Guild, and R. A. Armstrong. 2012. Hyperspectral distinction of two Caribbean shallow-water corals based on their pigments and corresponding reflectance. Remote Sens. **4**: 3813–3832.

H. Dierssen, IOCCG 2016